Coastal Engineering 117 (2016) 176–190

Contents lists available at ScienceDirect

Coastal Engineering

journal homepage: www.elsevier.com/locate/coastaleng

A new parameterisation for runup on gravel beaches

Timothy G. Poate [a,*], Robert T. McCall [b], Gerd Masselink [a]

[a] School of Marine Science and Engineering, Faculty of Science and Technology, Drake Circus, Plymouth, Devon PL4 8AA, United Kingdom
[b] Deltares, Rotterdamseweg 185, Delft, 2629, HD, The Netherlands

ARTICLE INFO

Article history:
Received 26 January 2016
Received in revised form 26 April 2016
Accepted 3 August 2016
Available online 2 September 2016

Keywords:
Gravel
Runup
XBeach
XBeach-G
Beaches
Barriers
Video
Parameterisation

ABSTRACT

Video derived runup statistics from ten separate deployments at six field sites have been used to develop a new parameterisation for the prediction of runup of runup on gravel beaches. These data were collected over a 2-year period under energetic storm conditions with significant wave heights of H_s = 1–8 m from gravel beaches and barriers composed of fine gravel (D_{50} = 2 mm) to large pebbles (D_{50} = 160 mm). An additional data set was generated using the numerical model XBeach-G, developed specifically for gravel beaches, and this synthetic dataset was used to further explore the role of hydrodynamic and morphological parameters on wave runup. A runup equation was developed using the synthetic data set and validated using the field data. The four parameters in this equation are, in decreasing order of importance, significant deep water wave height (H_s), spectral mean period ($T_{m-1,0}$), beach slope ($\tan\beta$) and grain size (D_{50}). The new gravel beach runup equation was found to fit the synthetic data set and the field data extremely well (r^2 = 0.97 and 0.89, respectively) and the new equation performs significantly better than existing runup equations, even those specifically developed for gravel beaches.

1. Introduction

Gravel beaches and barriers are large morphodynamic features that are common along many formerly glaciated and para-glaciated coasts (e.g., northern Europe, Canada) and along coasts backed by high mountainous terrain where gravel is supplied by local rivers (e.g., Mediterranean, New Zealand). Composed of coarse sediment (D_{50} > 2 mm), the beaches generally support steep profiles ($\tan\beta > 0.1$) and, in the absence of cliffs, are often backed by low-lying land, freshwater lagoons and/or estuaries. While reflective gravel beaches provide an effective coastal defence during elevated water levels and storm conditions, and are considered sustainable forms of coastal defence (e.g., Johnson, 1987; Aminti et al., 2003), they can undergo rapid and large-scale changes in their morphology (Orford et al., 2003). While complete barrier breakdown is rare, the characteristic, low-lying back barrier region can suffer rapid inundation under such conditions, and this can be of significant concern for coastal managers.

The morphological response of gravel beaches to changes in extreme hydrodynamic forcing has been well studied (Orford et al., 1991; Orford et al., 2003) and storm response can be grouped into four main regimes – swash, overtopping, overwashing and breaching – which represent increased wave, water level and runup conditions. The main controlling aspect of barrier response is the elevation difference between the runup and the barrier crest, which is known as 'freeboard'. When the runup level does not exceed the crest of the gravel barrier (i.e., positive freeboard), the seaward face of the beach will be subjected to energetic swash processes that can significantly alter the beach morphology, but leaves the crest untouched (Ruiz de Alegria-Arzaburu and Masselink, 2010). As the runup level starts to exceed the crest level (i.e., negative freeboard), sediments get transferred from the front of the barrier to the barrier crest and sediment deposition can lead to vertical accretion of the crest in a process termed overtopping (Orford and Carter, 1982). As the runup level and swash flows increase even more, overtopping is replaced by overwashing, resulting in sediment deposition on the landward slope of the beach/barrier (Orford et al., 1991). Sediment can be sourced from the barrier crest, leading to lowering of the barrier crest which enhances overwashing even more through positive feedback (Matias et al., 2012). Continued overwash, on the shorter term as a result of a very extreme event with large negative freeboard and on the longer-term aided by sea-level rise, can lead to barrier rollover (landward migration of the barrier system) or even barrier break-down (Orford et al., 1991). Barrier morphology, sediment characteristics (composition, permeability, sediment availability) and forcing conditions all influence the rate of barrier migration and the long-term barrier resilience.

During the 2013/2014 winter, the southwest coast of England experienced several extreme storm events that resulted in barrier overwash at several sites, including Chesil Beach and Hurst Spit in Dorset, Slapton Sands and Westward Ho! in Devon, and Loe Bar in Cornwall (Masselink et al., 2015). The key factors controlling the occurrence of overwashing is the maximum runup level, which is summation of tide, storm surge and wave runup; therefore, the ability to predict runup due to waves is a very useful coastal engineering application. Accurate estimation of

* Corresponding author.
E-mail addresses: timothy.poate@plymouth.ac.uk (T.G. Poate), Robert.mccall@deltares.nl (R.T. McCall), Gerd.masselink@plymouth.ac.uk (G. Masselink).

http://dx.doi.org/10.1016/j.coastaleng.2016.08.003

runup provides increased capabilities for vulnerability assessment and also assists with the effective design for nourished gravel beaches (Stripling et al., 2008).

The logistical challenge of measuring wave runup on gravel beaches, especially under energetic wave conditions, has meant that sandy beaches have been the main focus for field observations of wave setup and runup over the last decades (e.g., Guza and Thornton, 1982; Holman, 1986; Nielsen and Hanslow, 1991; Ruessink et al., 1998; Ruggiero et al., 2001; Stockdon et al., 2006). Field studies have been undertaken using a range of methodologies, including in-situ logging using resistance runup wire (Holman and Guza, 1984) and remote techniques involving video cameras (Holman and Sallenger, 1985). Such observations have formed the basis for formulating equations for predicting runup extent and behaviour on beaches (Holman and Sallenger, 1985; Stockdon et al., 2006) and solid structures (Van der Meer and Janssen, 1994; Hughes, 2004). One of the most commonly cited and effective predictors for sandy sites is by Stockdon et al. (2006), who used data from a range of reflective to dissipative beaches to develop an empirical parameterisation for runup based on wave height, wave period and beach gradient. This equation is widely used for predicting the overwash potential on and vulnerability of sandy barrier islands during extreme storm events (e.g., Stockdon et al., 2007). While Stockdon et al. (2006) provides formulae for more reflective sites, no data from gravel beach sites was included in the development of the runup equation. Application of the Stockdon et al. (2006) equation to several gravel beach sites in the UK suggests that wave runup on gravel beaches under energetic wave conditions is significantly under-predicted by the equation (Masselink et al., 2015), although the equation did perform quite well in a large scale flume experiment involving a gravel barrier forced with relatively calm conditions (Matias et al., 2012).

The unsatisfactory application of sandy beach runup formulae to gravel beaches is a reflection of some fundamental differences in morphodynamics between beaches made of sand and gravel (Buscombe and Masselink, 2006). The most important difference is related to the steeper profile of gravel beaches and their ability to maintain a reflective profile under extreme wave conditions (Hughes and Cowell, 1987) through adjustments to the beach step (Austin and Masselink, 2006; Austin and Buscombe, 2008; Ivamy and Kench, 2006). This difference becomes especially relevant under energetic wave conditions. On sandy beaches, runup under extreme wave conditions becomes dominated by infragravity waves (Guza and Thornton, 1982; Holman and Sallenger, 1985; Ruessink et al., 1998; Ruggiero et al., 2001; Stockdon et al., 2006; Senechal et al., 2011) with the incident storm waves simply breaking and dissipating their energy further offshore, whereas on gravel beaches very large waves can directly impact on the beach (Fig. 1). It is important in this context to distinguish between the three major types of gravel beaches, as identified by Jennings and Shulmeister (2002). Both the 'mixed sand and gravel' and 'composite gravel' beach types are likely to develop a dissipative surf zone under energetic wave conditions; however, the 'pure gravel' beach type is the one most likely to retain its reflective status during storms.

There are runup equations specifically derived for gravel beaches. In the UK, Powell (1990) used field measurements of gravel beaches in combination with a physical model to develop a runup predictor for gravel beaches. However, while the Powell (1990) equation is designed for gravel sites, the beach slope is represented only through the sediment size, potentially limiting its use. More recently, Polidoro et al. (2013) used field measurements on gravel beaches to develop an improved runup formula, but these were quite specific to the beaches along the southeast coast of England where mixed sand and gravel beaches are dominant and a bimodal wave climate prevails. The equation by Polidoro et al. (2013) also requires a large number of wave parameters that are not always available, making it less straightforward to use. Neither the Powell (1990) nor Polidoro et al. (2013) equations have been developed using extreme wave conditions and their application to very large waves ($H_s > 5$) would require extrapolating their use beyond conditions for which they were developed.

In summary, there is a lack of field measurements of wave runup on gravel beaches under energetic waves and such data are required to develop robust runup predictors specific to such environments and conditions. This paper addresses this lack by presenting field data collected from six gravel-dominated field sites ($D_{50} = 2$–150 mm) during ten periods of energetic conditions ($H_s = 1$–8 m) with the principal aim to propose a new runup parameterisation specific to (pure) gravel beaches. We will first describe the methods employed during these field campaigns and the processing undertaken to derive runup statistics, and compare these with existing runup formulations. We then use the numerical model XBeach-G (McCall et al., 2014; Masselink et al., 2014; McCall et al., 2015a), a gravel-specific development of the XBeach model (Roelvink et al., 2009), to firstly compare our field data to the XBeach-G model and then use the model to generate synthetic data to extend and explore the parameter space beyond that represented in the field. Both field data and synthetic data are also compared to existing runup formulations. A new wave runup equation is then developed from the XBeach-G data and validated using the field data.

2. Methodology

2.1. Field sites

The collection of in-situ runup datasets and corresponding morphological response was undertaken at six gravel beaches across southern

Fig. 1. Wave breaking directly on Chesil beach during storm on 5 February 2014; the flow just landward of the large collapsing breaker is best described as backwash. (photo by Richard Broome, reproduced with permission).

and northern England during ten deployments: Seascale (SEA), Westward Ho! (WWH), Loe Bar (LOB); Slapton Sands (SLP); Chesil (CSL) and Hayling Island (HGI). Seascale is a dissipative low tide sandy beach (350 m cross-shore) with a steeper ($\tan\beta = 0.07$) gravel ($D_{50} = 2$ mm) upper beach backed by a dune. Located in the Irish Sea, the site is sheltered from larger Atlantic swells and the storm climate is instead dominated by short duration wind sea events (Figs. 2A, 3A). Westward Ho! is similar to Seascale with a large dissipative sandy beach (500 m cross-shore) backed by a large pebble ridge. The steep barrier ($\tan\beta = 0.26$ consist of cobble-sized clasts ($D_{50} = 160$ mm) and protects the low-lying nature reserve inland from flooding. The beach is exposed to Atlantic storm systems (Figs. 2B, 3B) although the sandy low tide beach creates a wide dissipative surf zone during storm events, limiting swash energy on the gravel beach. Loe Bar, described in more detail in Poate et al. (2013), is a gravel barrier (250 m cross-shore, 500 m alongshore) backed by a freshwater lagoon and forms part of a 3-km long section of gravel coastline. The barrier is composed of fine gravel ($D_{50} = 30$ mm), with dominant cuspate morphology, and $\tan\beta$ is 0.12. The beach faces south west and is exposed to the dominant Atlantic swells (Figs. 2C, 3C). Slapton Sands is an 80–120-m wide and 4.5-km long gravel barrier system, and is also backed by a freshwater lagoon. The beach is composed of fine gravel ($D_{50} = 2$–10 mm) and $\tan\beta$ is 0.13. Slapton Sands faces southeast and is partly protected from Atlantic swells by Start Point which lies to the south (Figs. 2D, 3D). The beach mainly experiences easterly storm waves and southerly Atlantic swell traveling up the English Channel (Ruiz de Alegria-Arzaburu and Masselink, 2010). Chesil beach extends for 18 km and is 200 m wide, and is also backed by a fresh water lagoon. The grain size varies considerably along the beach, but $D_{50} = 40$–60 mm at the measurement site. For the two deployments at Chesil, the barrier slope was $\tan\beta = 0.2$ and 0.4 making it the steepest of the measurement sites. Facing southwest, the beach is exposed to dominant Atlantic swells and more localised wind seas (Figs. 2E, 3E). The final site, Hayling Island, is composed of a mixture of sand and gravel ($D_{50} = 20$ mm) and $\tan\beta = 0.10$. Due to the relatively low crest elevation, the beach is susceptible to coastal flooding during storm events coinciding with spring tides. Located relatively far up the English Channel and in the lee of the Isle of Wight, the beach is sheltered from swells traveling up the channel (Figs. 2F, 3F). With reference to the gravel beach types of Jennings and Shulmeister (2002), Hayling Island represent a mixed sand and gravel beach, Seascale and Westward Ho! are composite gravel beaches and Loe Bar, Slapton Sands and Chesil are pure gravel beaches.

2.2. Data collection

Survey dates, site characteristics and wave conditions for all field deployments are summarised in Table 1. The field deployments were centred around periods of energetic/storm conditions to provide a wide range of runup values for each site. The longest deployment, LOB1, took place in March 2012 and formed part of a larger field experiment, described in detail by Poate et al. (2013), concerning bed-level dynamics under energetic waves. The other deployments were conducted over one to four days, designed to capture a specific period of storm conditions.

At each site, wave runup was measured using video data logged using a temporary camera installation (Fig. 4), in line with pixel stack methods described by Holland et al. (1995). The cameras used were Pointgrey Grasshoper 2MP with 8, 12 and 25 mm lenses, depending on the site. Individual frames were collected at 3.75 Hz and time stamped by the host PC which was synchronised with a GPS clock. Measured three-dimensional morphology (using real time kinematic GPS) from the preceding low water was used to define and extract three alongshore profile lines within the image and these were used to construct pixel stacks. Pixel stacks were sampled at 3.75 Hz for 17-min periods to reduce tidal translation during the stack and to maximise the dataset per site.

Following Stockdon et al. (2006), the leading edge of the runup maxima was extracted using a threshold exceedance approach to detect the transition from beach to water (Fig. 4). The digitized waterline, once checked for accuracy, was then converted to both local elevation and cross-shore position with reference to the morphology that was used to define the pixel line (Fig. 4). Measured local tide data, from outside the surfzone, were used to reduce the vertical swash excursions to elevation

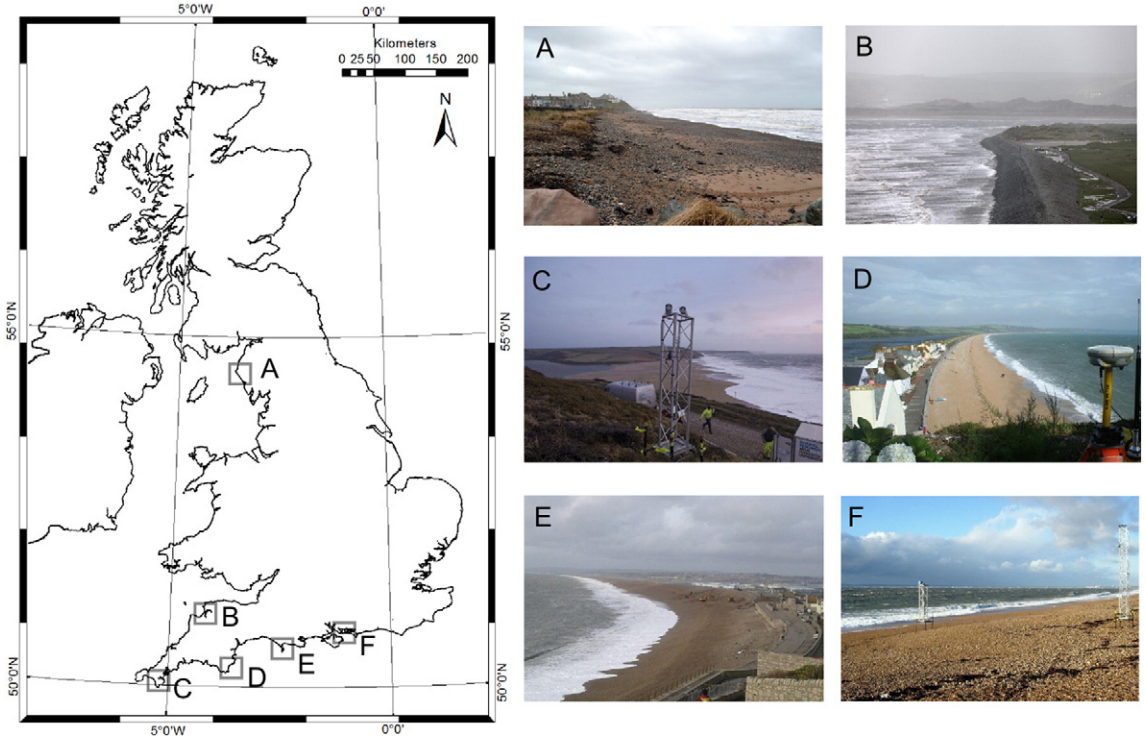

Fig. 2. Location and photographs of the field sites: A = Seascale (SEA); B = Westward Ho! (WWH); C = Loe Bar (LOB); D = Slapton Sands (SLP); E = Chesil (CSL); and F = Hayling Island (HGI).

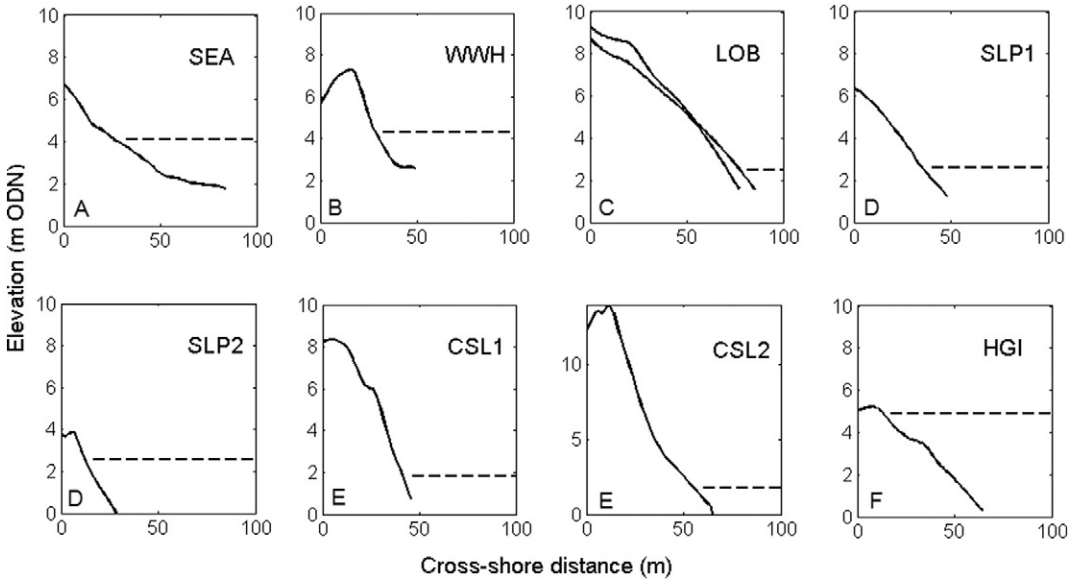

Fig. 3. Representative profiles of the six field sites listed in Table 1. Horizontal dashed lines indicate Mean High Water Springs (MHWS) and ODN (Ordnance Datum Newlyn), which represents the water level reference datum in the UK (c. 0.2 m above current MSL). Note the different vertical scale for CSL2.

above a still water level. The leading edge of the uprush of the swash is a distinctive feature which can be easily extracted through automated routines, with minimal human input; however, the downrush is less clear, limiting delineation of its position under storm waves. Therefore, no estimates were made of the wave setup or variability of the swash excursion (cf. Holman and Sallenger, 1985; Stockdon et al., 2006).

The elevation and location of the cameras has an impact on the cross-shore resolution of the pixel stack extracted and varied between the different deployments (Holman and Guza, 1984; Holland et al., 1995). The vertical resolution was 0.1–0.2 m and the horizontal resolution was 0.25–0.65 m; this is in line with previous studies (Holland et al., 1997). Runup statistics were calculated for each 17-min period with a 2% exceedance value derived from the cumulative probability density function of runup maxima elevations (Stockdon et al., 2006). The beach slope ($\tan\beta$) was calculated for each 17-min period using the part of the profile extending from the still water level plus the significant wave height (SWL + H_s), down to the lower limit of the still water level minus twice the significant wave height (SWL − $2H_s$).

2.3. Environmental conditions

Nearshore wave data are provided by Datawell MKIII Directional Waveriders owned and managed by the Channel Coastal Observatory for all sites except SEA where wave data was provided by CEFAS. The buoys are deployed in ~10 m Chart Datum and provide half-hourly wave statistics accessible online. The raw spectral files from the buoys were used to compute the spectral moments which were used to calculate the spectral mean wave periods:

$$T_{m0,1} = m_0/m_1 \tag{1}$$

$$T_{m0,2} = \sqrt{m_0/m_2} \tag{2}$$

$$T_{m-1,0} = m_{-1}/m_0 \tag{3}$$

where $T_{m0,1}$ is based on the first positive moment of the energy spectrum, $T_{m0,2}$ is based on the second positive moment and $T_{m\ -\ 1,0}$ is based on the first negative moment of the energy spectrum. Local tide data were collected using an RBR TWR 2050 pressure sensor deployed at low water. Tidal curves were produced using average values collected over 2 min at a rate of 4 Hz every 15 min. Water level data were corrected for local atmospheric pressure using a nearby meteorological station to each site.

Measured runup statistics are compared with runup equations proposed by our data with previous work by Powell (1990); Van der Meer and Janssen (1994); Stockdon et al. (2006) and Polidoro et al. (2013), and these will be referred to as Powell1990, Meer1994, Stockton2006 and Polidoro2013 for the remainder of this paper. The runup equations are provided in Appendix A and the variables used have been kept

Table 1
Summary of the field site characteristics during storm events. In the case of SEA and WWH, † refers to the upper gravel beach only. Beach slope ($\tan\beta$), grain size (D_{50}), significant wave height (H_s), tide range (TR), hydraulic conductivity (K), peak wave period (T_p) and mean wave period (T_z).

Site		Date	Site conditions					Measurement conditions		
			$\tan\beta$ (−)	D_{50} (mm)	$H_{s10\%}$ (m)	TR (m)	K (ms^{-1})	Max H_s (m)	Max T_p (s)	Peak T_z (s)
A	SEA	27–31 Jan. 2013	0.07	2	1.3	5.5	0.02†	2.8	7	5.5
B	WWH	2–3 Nov. 2013	0.26	160	1.8	7.3	0.50†	6	15	9
C	LOB1	Mar 2012	0.12	3	2.4	3.1	0.003	2.5	12	7
	LOB2	20–24 Nov. 2012	0.12	3	2.4	3.1	0.003	5.8	12	7
	LOB3	1–2 Feb. 2014	0.12	3	2.4	5.7	0.003	5	20	7.5
D	SLP1	21–22 Feb. 2013	0.13	2	1.4	2.2	0.075	2	7	6
	SLP2	20–22 Oct. 2013	0.15	10	1.4	4.2	0.075	2	12	6
E	CSL1	14–17 Dec. 2012	0.20	50	1.9	3	0.40	4	10	5
	CSL2	4–6 Feb. 2014	0.40	50	1.9	4.4	0.40	8	22	10
F	HGI	27–28 Oct. 2013	0.10	20	1.2	2	0.075	3.8	19	6

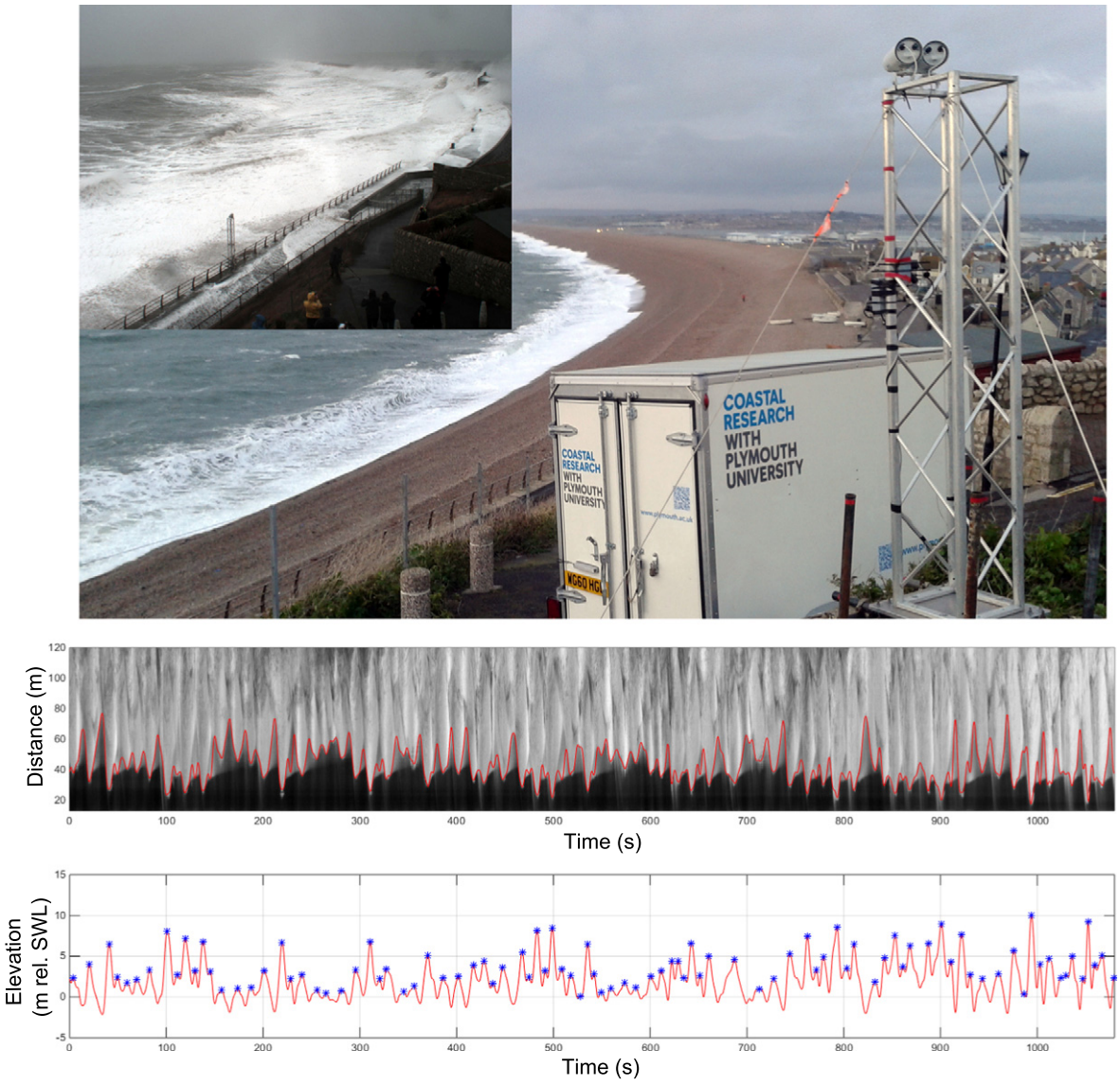

Fig. 4. Mobile camera deployment with camera tower and data logging unit in the foreground and the Chesil gravel barrier (~18 km long) in the background (top panel). The inset image shows the camera view during one of the storm events. Lower panels show automated runup position extracted from 17-min timestack (red line) and individual vertical swash extent with reference to the still water level (blue asterisk).

consistent with the original publications to aid interpretation. The peak wave period (T_p) and the spectrally derived wave periods ($T_{m-1,0}$ and $T_{m0,2}$) were used as defined in the original papers. All runup equations require the deep water wave height, whereas only wave heights from intermediate water depth (h = 10–20 m) were available. The deep water wave height (H_o) was obtained by de-shoaling the nearshore significant wave height using the spectral mean period to 200 m water depth. The peakedness of the wave spectrum was defined as;

$$Q_p = \frac{2}{m_0}\int f S_f^2 df \tag{4}$$

where S_f is the one-dimensional frequency-energy density spectrum and f is the frequency (Goda, 1976). Bimodality was computed as the ratio of $T_{m-1,0}/T_{m0,1}$ with results > ~1.15 representing bimodal sea states. The measured runup statistics are also compared by predictions of the XBeach-G model and the newly-derived runup equation based on synthetic runup data obtained with the model (see below). In the comparison of measurement data to model results and the new equation the statistical measures r^2 (coefficient of determination) and bias have been used.

$$\text{bias}(x) = \frac{1}{n}\sum_{i=1}^{n}\left(x_{i,\text{modelled}} - x_{i,\text{measured}}\right) \tag{5}$$

2.4. XBeach-G

The XBeach-G model (McCall et al., 2014; Masselink et al., 2014; McCall et al., 2015a) is first used to hindcast wave runup during the storm events listed in Table 1. The model results are compared to measurements of runup and to runup predictions made by the four runup equations. XBeach-G is a 1D (depth-averaged, cross-shore) process-based model that solves intra-wave flow and surface elevation variations for waves in intermediate and shallow water depths, as well as infiltration and exfiltration on the beach face. The model hydrodynamics have previously been validated for use on pure gravel beaches using physical model data and field measurements (McCall et al., 2014).

Wave runup hindcasts are carried out for the storm events in Table 1 in a manner similar to that described by McCall et al. (2014). For each

storm event, one XBeach-G simulation is run for every 1–3 sequential daytime high-tides of the storm. Each high-tide simulation is run for the duration of maximum tide levels and contiguous camera data, which was generally in the order of 1 h.

The XBeach-G hindcast simulations are forced using time series of wave spectra measured at the nearest wave buoy, described in the previous section, and measured tide and surge levels. The model uses the input wave spectra to generate a random time series of incident waves and bound low-frequency second order waves at the model boundary. To quantify the sensitivity of the modelled runup levels to the selection of random wave components at the model boundary, each XBeach-G storm hindcast is run ten times using a new random wave time series of the imposed offshore wave spectrum. The hydraulic conductivity of the beach used to compute infiltration and exfiltration rates in the model is given for all sites in Table 1.

XBeach-G is subsequently used to generate a synthetic dataset of wave runup under varying environmental conditions and this data set will be used to derive a new runup equation, specific to gravel beaches. For this analysis, 14,779 XBeach-G simulations are run on an idealised planar gravel beach profile with sufficient height to never be overtopped by waves (Fig. 5). Every XBeach-G simulation is run to generate one value of wave runup from 1 h. of shoreline elevation data, using one constant still water level (SWL) and one wave spectrum. Variations between runs are generated by selecting random values from a uniform distribution of the beach slope tanβ, median grain size D_{50}, and parameters of the wave spectrum (Table 2).

Previous work along the south coast of England has suggested that wave runup is affected by wave bimodality; specifically, bimodal wave spectra lead to larger runup (Stripling et al., 2008; Polidoro et al., 2013) and potentially more significant beach profile response during storm events (Bradbury et al., 2007). The role of bimodality is explored by including both unimodal (N = 7362) and bimodal (N = 7417) wave spectrum forcing in the XBeach-G simulations for the synthetic runup dataset. In the case of bimodal spectra, the secondary spectral peak is related to the randomly-drawn primary peak through scaling of the primary wave period and wave height, where the scaling factor is again drawn from a uniform random distribution (Table 2). All wave spectra are imposed with normally-incident wave direction, a JONSWAP peak enhancement factor of 3.3, and a directional distribution of 27 degrees.

To minimize the parameter space to be investigated and to remove unlikely and unnatural combinations of geotechnical parameters, the hydraulic conductivity of the beach face K is related to the square of the grain size (cf. Hazen, 1892). Using values for K found at Loe Bar (Austin et al., 2013) and Chesil Beach (Heijne and West, 1991) as reference values in the fine and coarse gravel range, we define a parabolic function for the hydraulic conductivity used in the synthetic dataset generation (cf. McCall et al., 2015b):

$$K = 244D_{50}^2 + 0.01 \qquad 0.002 \le D_{50} \le 0.050 \tag{6}$$

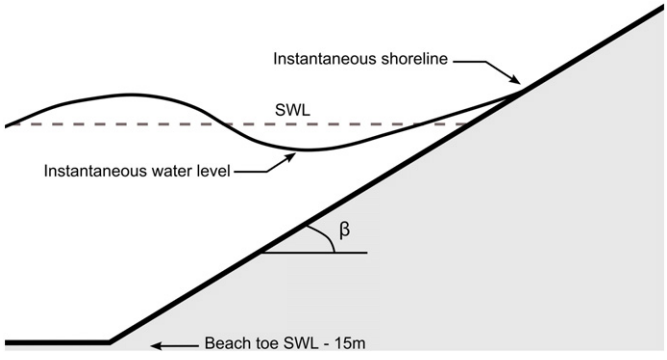

Fig. 5. Schematic of the idealised gravel beach profile used to generate the XBeach-G runup dataset.

In all simulations, the cross-shore resolution of the XBeach-G models is set to vary gradually in the cross-shore direction, from ~1 m at the offshore boundary of the model, to ~0.1 m near the waterline in order to correctly capture wave breaking and wave runup in the model.

For the purpose of this study, the most landward extent of the swash with a water depth of at least 0.01 m is defined in the model as the shoreline position (cf. McCall et al., 2015a). The time series of the modelled shoreline position is subsequently analysed in the same manner as the shoreline from the camera pixel stacks to compute runup exceedance levels.

3. Results

3.1. Description of field data

The variability in measured runup between the sites is given in Fig. 6 which compares the significant wave height (H_s) and the 2% exceedance runup value ($R_{2\%}$) for all 17-min data segments (N = 1466). The most energetic wave conditions were experienced during the LOB3 and CSL2 experiments with H_s exceeding 4 m and 6 m, respectively, generating $R_{2\%}$ of >6 m and 8 m, respectively. The relative runup height (ratio between runup and wave height: $R_{2\%}/H_s$) varies between the sites: for CSL2 and LOB3, $R_{2\%}/H_s$ is c. 1.8; for SLP, $R_{2\%}/H_s$ is c. 1; and for HGI, WWH and SEA, $R_{2\%}/H_s$ is c. 0.5. These different $R_{2\%}/H_s$ ratios cause widely varying values for $R_{2\%}$ under similar wave conditions. For example, for H_s = 5 m, $R_{2\%}$ is typically 10 m, 7 m, 5 m and 2 m for CSL2, LOB3, LOB2 and WWH, respectively (Fig. 6).

For some locations, $R_{2\%}/H_s$ also depends on the wave conditions. At WWH and SEA, there is a point when the ratio $R_{2\%}/H_s$ decreases with increasing wave conditions; this is expected given the wide dissipative nature of the lower profile at these sites and the steep upper gravel section of the profile (Fig. 3). Under energetic conditions, wave breaking will take place over the low gradient, sandy part of the beach profile, limiting wave runup on the steep gravel part of the beach.

The Iribarren number or the surf similarity parameter ξ_o (Battjes, 1974) is a dimensionless parameter that has been used widely to describe beach and surf zone morphodynamics and frequently features in runup predictors (e.g., Battjes, 1971; Roos and Battjes, 1976; Holman and Sallenger, 1985; Holman, 1986; Van der Meer and Stam, 1992; Stockdon et al., 2006).

$$\xi_o = \frac{\tan\beta}{\sqrt{H_o/\lambda_o}} \tag{7}$$

where

$$\lambda_o = gT^2/2\pi \tag{8}$$

and tanβ = beach slope, H_o = deep water wave height, λ_o = deep water wavelength, $T = T_{m-1,0}$ (wave period), g = acceleration due to gravity, and the subscript '$_o$' denotes deep water conditions.

Plotting the relative runup $R_{2\%}/H_s$ versus the Iribarren number ξ_o allows exploration of the runup data within a morphodynamic parameter space (Fig. 7) and generally shows an increased value for $R_{2\%}/H_s$ as conditions become more reflective. An early runup predictor by Holman and Sallenger (1985) simply considered $R_{2\%}/H_s = 0.92\xi_o$, and this fits the data reasonably well, albeit with a large amount of scatter. Fig. 7 also includes the runup predictor by van der Meer and Stam (1992), who identified the role of surface roughness on runup by observing that runup on a smooth surface is approximately twice that of a rough surface. Most of the field data is quite well constraint by the two curves of van der Meer and Stam (1992), but a large amount of data from the intermediate domain (LOB1 and LOB2) plots significantly above the smooth-slope curve. For most sites, the majority of the data is characterised by $R_{2\%}/H_s > 1.5$, but $R_{2\%}/H_s < 1.5$ for WWH and SEA,

Table 2
Overview of input random parameter distributions within XBeach-G runup dataset (N = 14,779). The parameter s is the deep water wave steepness, defined as $s = H_{m0}/L_{p,0}$, and in the case of bimodal spectra, the subscript p represents the primary wave peak and the subscript s represents the secondary higher (wind wave) or lower (swell wave) peak.

Beach properties	$\tan\beta$ (−)	D_{50} (mm)			
	U (0.05,0.20)	U (2,50)			
Unimodal spectrum properties	H_s (m)	s (−)			
	U (2,6)	U (0.01,0.05)			
Bimodal spectrum properties	$H_{s,p}$ (m)	s_p (−)	$H_{s,s}$ (m)	$T_{p,s}$ (s) ($T_{p,p} < 10$ s)	$T_{p,s}$ (s) ($T_{p,p} > 10$ s)
	U (2,5)	U (0.01,0.05)	U (0,1) $H_{s,p}$	U (1.80,2.20) $T_{p,p}$	U (0.45,0.56) $T_{p,p}$

especially for the more energetic wave conditions. This is attributed to the dissipative nature of the lower part of the beach profile on these beaches. For this reason, the data collected from these two 'composite gravel' beaches have been excluded from the remaining analysis in the paper; the focus will remain on the 'pure' gravel sites SLP, CSL and LOB, and the 'mixed sand and gravel' site HGI. Attention will be focussed on high tide conditions during which wave breaking occurred directly on the beach.

3.2. Comparison of field data with existing equations

Existing studies of runup have focused on sandy beaches and impermeable structures under relatively low energy conditions. Using the measured hydrodynamic conditions and profile information, four existing runup equations (refer to the Appendix A for formulations) are applied to the measured runup values from our dataset for comparison (Fig. 8). Under low energy conditions the runup formulae show a reasonable fit with the measured results (Fig. 8); however, as the wave energy increases, all equations significantly under-predict by up to 50% the measured values. Powell1990 performs better under low energy conditions, compared to the other equations, with less data spread (Fig. 8). As pointed out in the introduction, there are, however, practical issues associated with the application of Polidoro2013 and Powell1990; therefore, it is considered appropriate to pursue with finding an new runup equation for gravel beaches, rather than modify an existing one.

3.3. Comparison of field data with XBeach-G

Parametric equations such as discussed in the previous section try to capture the complexity of the beach profile and the wave conditions in simple parameters to yield easily applicable runup predictors. More accurate runup predictions can be obtained using more sophisticated numerical models, but their implementation is less straightforward. Once a properly validated numerical model is available, however, the model can be used to generate simulated runup data that further populates sparse sections of the parameter space and these synthetic data can then be used in combination with field data to explore and develop improved parametric runup predictors.

The numerical model XBeach-G has been specifically developed to model hydrodynamics (McCall et al., 2014) and morphodynamics (McCall et al., 2015a, 2015b) for gravel beaches under energetic wave conditions. The ability of XBeach-G to predict runup observed on the six gravel beaches in Table 1 was tested through hindcasting 1-hour periods during the storm high-tides, as described in Section 2.4. This hindcast dataset represents a subset of the data shown in Fig. 7: only the two largest wave events during LOB1 are modelled (8 and 24 March 2012) and the model is only run for an approximate one-hour period during every daytime high-tide of the storm events listed in Table 1.

Mean measured and modelled 2% runup exceedance levels computed for every 15 to 20 min of simulation and measurement data are shown in Fig. 9. Vertical error bars associated with the data points

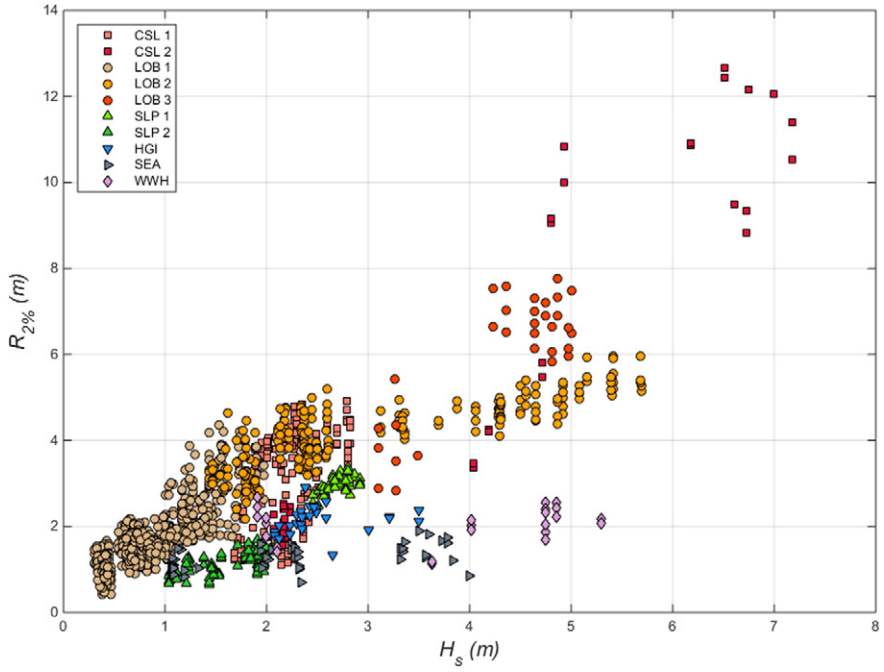

Fig. 6. Significant wave height (Hs) plotted against 2% runup exceedance ($R_{2\%}$) for the complete field data set (six sites and ten measurement periods).

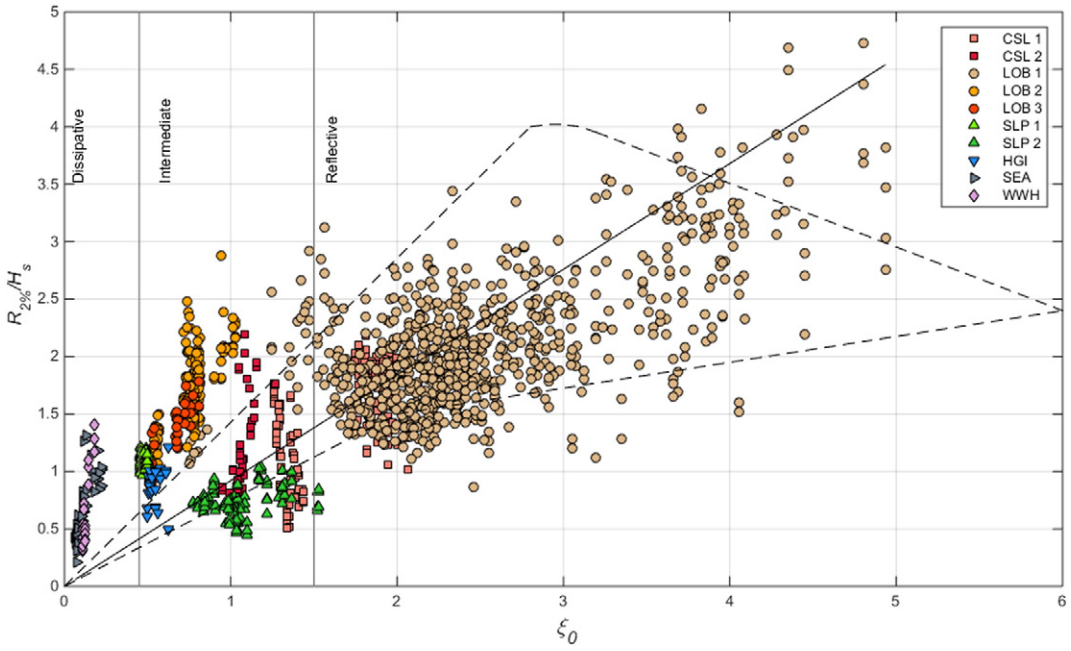

Fig. 7. Ratio of 2% exceedance (R2%) and the significant wave height (Hs) plotted against the Iribarren number (calculated using the offshore wave height) for the ten datasets. The dashed black line delineates previous runup spread for smooth slopes (upper line) and rock slopes (lower line) after van der Meer and Stam (1992). The solid black line shows the fit for 0.92ξo after Holman and Sallenger (1985). The vertical lines delineate reflective, intermediate and dissipative surf zone conditions and are based on Guza and Inman (1975).

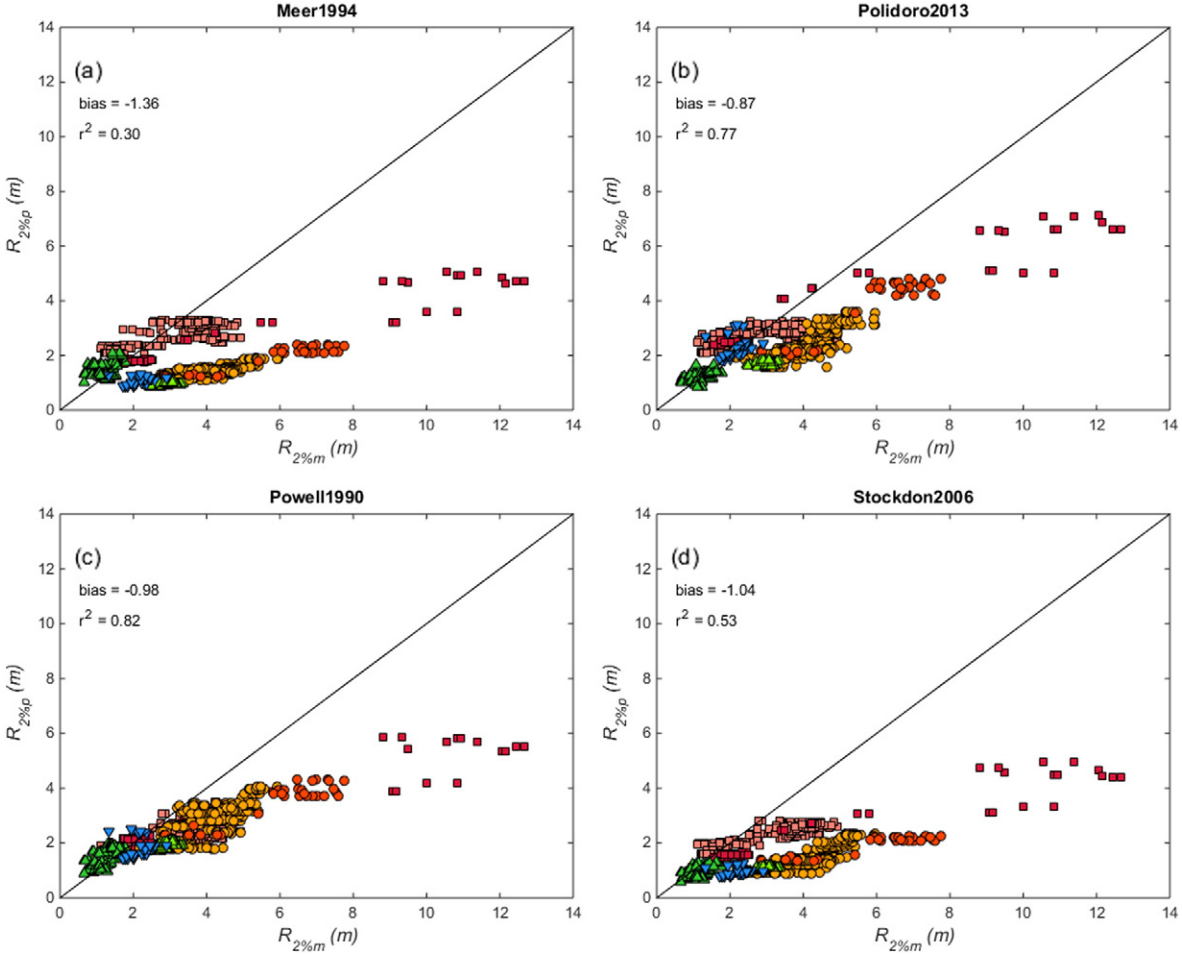

Fig. 8. Comparison between measured runup values ($R_{2\%m}$) and those predicted ($R_{2\%p}$) using the formulae outlined in Appendix A: (a) Meer, 1984; (b) Polidoro, 2013; (c) Powell, 1990; and (d) Stockdon, 2006. Symbol colours represent different sites and are consistent with Figs. 6 and 7.

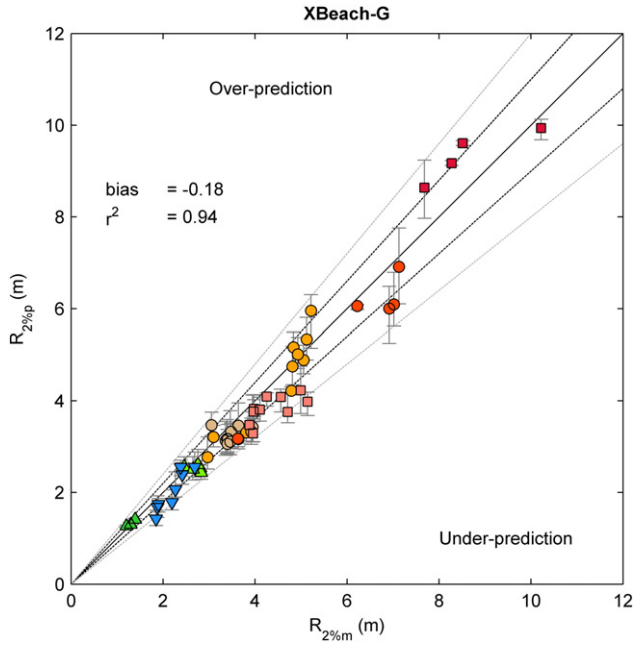

Fig. 9. Comparison of 2% exceedence runup between XBeach-G model ($(R_{2\%p})$) and field measurements ($(R_{2\%m})$). Black dashed line is the 10% error band while grey dashed line is the 20% error band. Symbol colours are consistent with Figs. 6 and 7.

represent variations in the modelled runup levels due to variations in the random wave time series applied at the model boundary (each XBeach-G storm hindcast is run ten times using different random wave time series drawn from the offshore wave spectrum). Horizontal error bars represent the minimum and maximum measured runup data across multiple cross-shore camera pixel stacks. The figure shows excellent agreement between modelled and measured $R_{2\%}$ values, with little scatter ($r^2 = 0.94$) and low bias (−0.14 m). The overall median relative error of the run-up hindcast is <10%, and 90% of the predictions have an error <23%. Performance of the XBeach-G model (Fig. 9) is vastly superior to that of the existing runup equations (Fig. 8).

3.4. Generating synthetic runup data with XBeach-G

XBeach-G was run 14,779 times on an idealised gravel beach (cf. Fig. 5) with varying random realisations of the beach slope tanβ, median grain size D_{50}, and parameters of the wave spectrum (Table 2) to generate a synthetic runup dataset. The resulting range of hydrodynamic and geotechnical parameters used in the XBeach-G synthetic runup dataset, as well as the range in runup and relative runup exceedance levels, are shown in Table 3.

The complete XBeach-G simulated runup data set is combined with the field data in Fig. 10, which simply plots the 2% exceedance runup height ($R_{2\%}$) versus the significant wave height (H_s). Although there is considerable overlap with respect to the $R_{2\%}$ and H_s parameter space between the modelled and measured data, the field data mainly represents the relatively low energy conditions ($R_{2\%} < 5$ m; $H_s < 3$ m), while the modelled data represents mainly high energy conditions. The model and field data overlap in the shared parameter space, except for the field data of SEA and WWH; as argued previously, these sites represent composite gravel beaches and are removed from the subsequent analysis.

In line with Fig. 8 the XBeach-G simulated dataset was compared against the four runup formulae (Fig. 11) to provide a further check against the measured data and the formulae performance. Again we see a consistent under-prediction, especially under energetic conditions, for each of the equations, with the exception of Powell1990 which exhibits distinctive data spread. The scatter shown reflects the fact that, unlike the other equations, Powell1990 ignores beach slope because it is assumed that this parameter is accounted for in the sediment size.

3.5. Developing a runup predictor based on synthetic data and validated using field data

The generation of an extensive synthetic dataset provides a valuable approach to explore a wide parameter space (cf. Table 3) to optimise a runup prediction tool. In line with Fig. 7, and approaches by Holman and Sallenger (1985) and Stockdon, 2006, the relationship between the relative runup ($R_{2\%}/H_s$) and the Iribarren number ($\xi_{m-1,0}$) is first explored in Fig. 12. In the figure, a relatively strong correlation is apparent between $R_{2\%}/H_s$, but by colouring the data points by the value of specific parameters it is clear that some of these parameters can provide additional explanatory power as visualised by the diagonal colour banding. Specifically, increased wave height and decreased sediment size appear to significantly enhance wave runup (Fig. 12a, d). Increased wave period and increased beach gradient also have a positive influence on wave runup, albeit less clear (Fig. 12b, c). The role of the spectral shape, as parameterised by bimodality ($T_{m-1,0}/T_{m0,1}$) and spectral peakedness (Q_p), is less evident (Fig. 12e, f).

To develop a new runup formula from the modelled data, $R_{2\%}$ and $R_{2\%}/H_s$ were first regressed against all relevant parameters on an individual basis and the most suitable exponent (n) for each was identified. The correlations are presented in Table 4 and demonstrate that $R_{2\%}$ is strongest correlated to H_s, closely followed by the wave period parameters. The other parameters play less important, but still significant roles. The key parameters were ranked in decreasing order of variance explained (r^2) and parameters were added as long as they significantly improved the fit with the model data. Note that since the hydraulic conductivity is not an independent variable in the synthetic runup dataset, but rather a function of the grain size, K is not included the regression analysis.

The resulting optimised runup equation for gravel beaches based on the synthetic data set is given by:

$$R_{2\%} = CD_{50}^{-0.15} tan\beta^{0.5} H_s T_{m-1m0} H_s \quad (9)$$

where the constant C = 0.21, and is dimensional (unit $m^{0.15}s^{-1}$). Eq. (9) is plotted in Fig. 13a against the runup data generated by XBeach-G, and appears appropriate across the full runup range ($R_{2\%}$ = 1–14 m) with limited bias (−0.13 m) and a high r^2 (0.97). Including any of the spectral shape parameters did not improve the equation and there does not seem to be any remaining bias in the data when the symbols are coloured with the value for bimodality or spectral peakedness (Fig. 13a). Detailed sediment size information is not always available and

Table 3
Overview of parameter space within XBeach-G runup dataset (N = 14,779). In this table, tanβ = beach slope, D_{50} = grain size, K = hydraulic conductivity, H_{m0} is the spectral significant wave height of the entire (unimodal, or bimodal) wave spectrum, Q_p is the spectral peakedness parameter of Goda (1976), and $\xi_{m-1,0}$ is the Iribarren parameter based on the deep water wave length related to the $T_{m-1,0}$ wave period, $R_{2\%}$ is the 2% exceedance runup.

	tanβ (−)	D_{50} (mm)	K (ms^{-1})	H_{m0} (m)	T_p (s)	$T_{m-1,0}$ (s)	$T_{m0,1}$ (s)	$T_{m-1,0}/T_{m0,1}$ (−)	Q_p (−)	$\xi_{m-1,0}$ (−)	$R_{2\%}$ (m)	$R_{2\%}/H_{m0}$ (−)
Min	0.05	2	0.01	2.00	5.11	4.67	4.40	1.06	1.41	0.20	0.37	0.18
Max	0.20	50	0.62	7.02	19.55	18.55	16.52	1.27	3.11	1.94	18.28	3.13

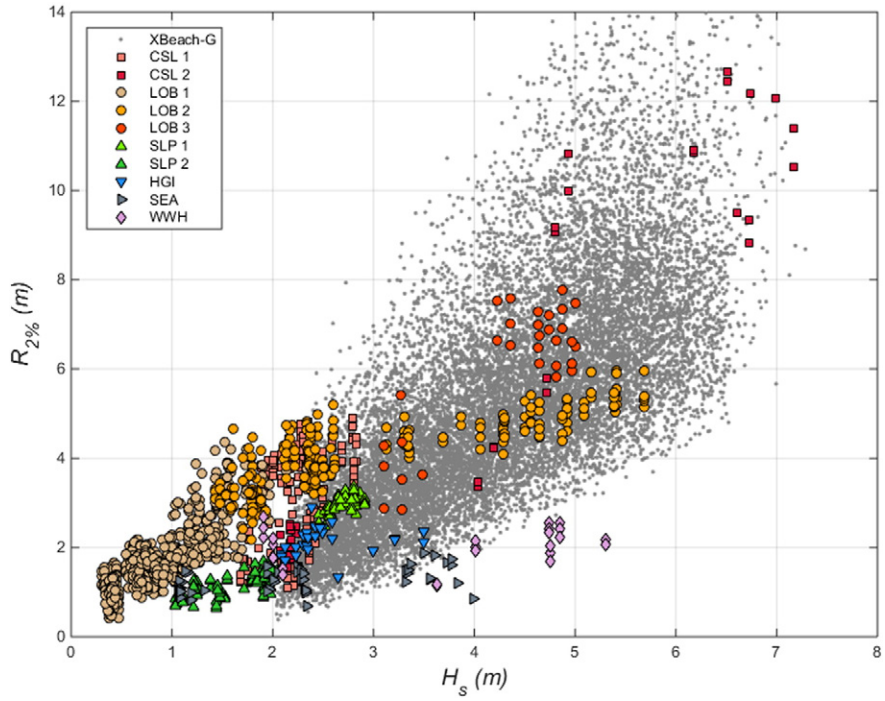

Fig. 10. Scatter plot of 2% runup exceedance ($(R_{2\%})$) and significant wave height ((H_s)) for XBeach-G generated dataset combined with measured field data.

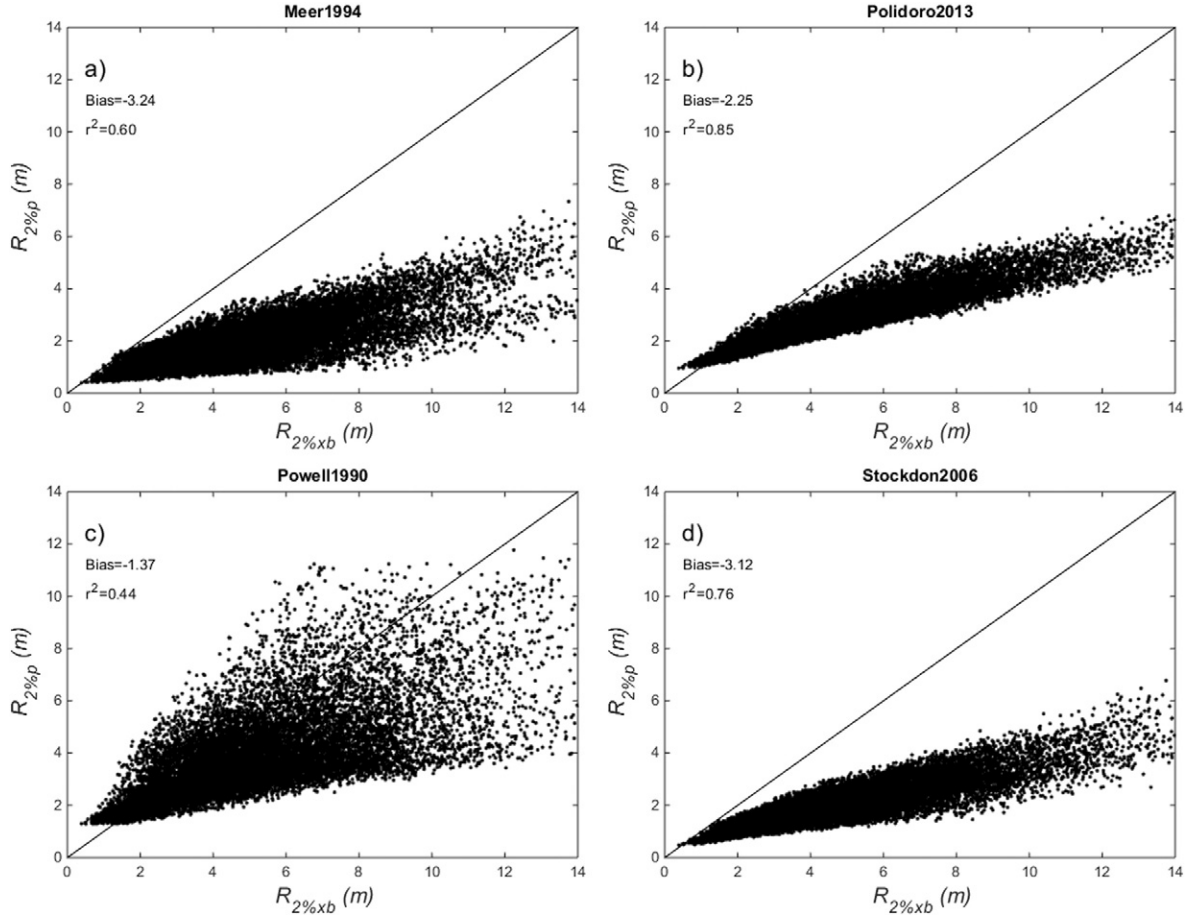

Fig. 11. Comparison between XBeach simulated runup values ($R_{2\%xb}$) and those predicted ($R_{2\%p}$) using the formulae outlined in Appendix A: (a) Meer, 1984; (b) Polidoro, 2013; (c) Powell, 1990; and (d) Stockdon, 2006.

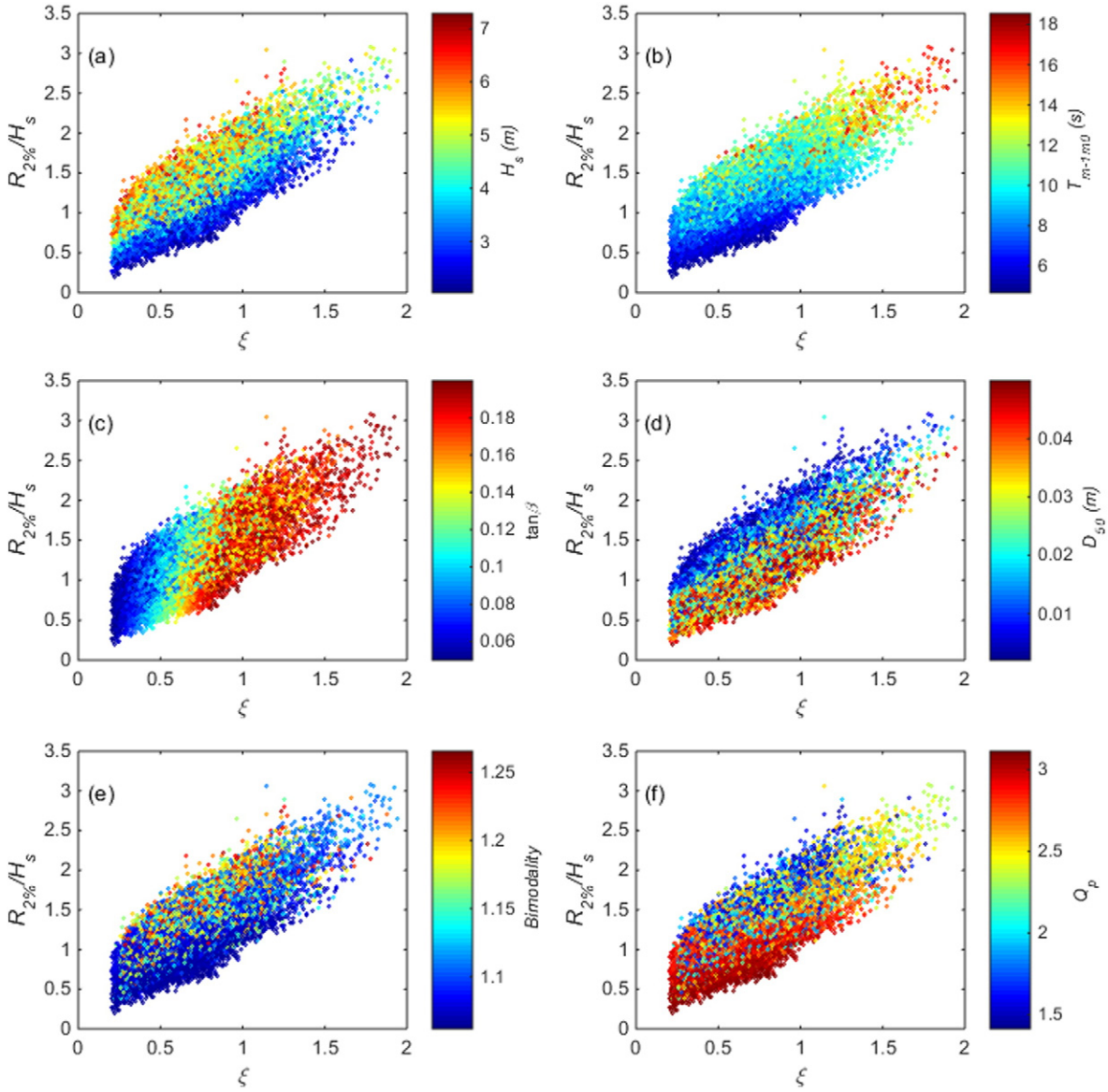

Fig. 12. Scatter plots of relative runup ($R_{2\%}/H_s$) and Iribarren number ($\xi_{m\text{-}1,0}$) with the colour of the symbols reflecting parameter values: (a) significant wave height (H_s); (b) spectral mean wave period ($T_{m\text{-}1m0}$); (c) beach slope (tanβ); (d) grain size (D_{50}); (e) bimodality ($T_{m\text{-}1,0}/T_{m0,1}$); and (f) spectral peakedness (Q_p).

sediment size is also highly spatially variable on gravel beaches. Eq. (9) was therefore simplified by leaving out D_{50} as a fitting parameter:

$$R_{2\%} = C\, tan\beta^{0.5} H_s T_{m-1m0} H_s \tag{10}$$

Table 4
Overview of regression analysis undertaken on XBeach-G runup dataset. In this table, tanβ = beach slope, D_{50} = grain size, H_s = significant wave height, T_z = mean wave period, T_p = peak wave period, Q_p = spectral peakedness parameter of Goda (1976), $\xi_{m-1,0}$ is the Iribarren parameter based on the deep water wave length related to the $T_{m-1,0}$ wave period.

	tanβ	D_{50}	H_s	T_p	T_z	$T_{m-1,0}$	$T_{m0,1}$	$T_{m-1,0}/T_{m0,1}$	Q_p	$\xi_{m-1,0}$
$R_{2\%}$ = f(variable)^n										
r^2	0.38	0.21	0.73	0.58	0.62	0.69	0.64	0.35	0.38	0.51
N	0.51	−0.15	1.47	1.26	1.66	1.66	1.68	4.34	−0.98	0.59
$R_{2\%}/H_s$ = f(variable)^n										
r^2	0.56	0.30	0.32	0.57	0.66	0.70	0.68	0.32	0.36	0.80
N	0.53	−0.14	0.47	0.77	1.06	1.05	1.07	2.68	−0.62	0.63

where C = 0.39 and, along with subsequent equations, is dimensional (unit s^{-1}). Eq. (10) is plotted in Fig. 13b and with an r^2 of 0.95 and a bias of 0.04 m still does a very good job in predicting the modelled runup heights. However, as evident by the distinct banding when the symbols are coloured on the basis of the D_{50} value, Eq. (10) significantly and systematically over-predicts runup for relatively coarse sediments and under-predicts for fine sediments.

To compute the wave period parameter $T_{m-1,0}$ requires knowledge of the complete wave spectrum (cf. Eq. (3)). However, this is not always available, either from measured wave data or modelled wave output; therefore, $T_{m-1,0}$ was replaced by T_z and T_p before the statistical analysis was repeated. The sediment size D_{50} was, again, omitted from the analysis, and the resulting runup equations are given by:

$$R_{2\%} = C \tan\beta^{0.5} T_z H_s \tag{11}$$

$$R_{2\%} = C \tan\beta^{0.5} T_p H_s \tag{12}$$

Eq. (11), where C = 0.49, (Fig. 13c) does a very good job and is very similar to Eq. (10) with regard to overall fit although there is notably

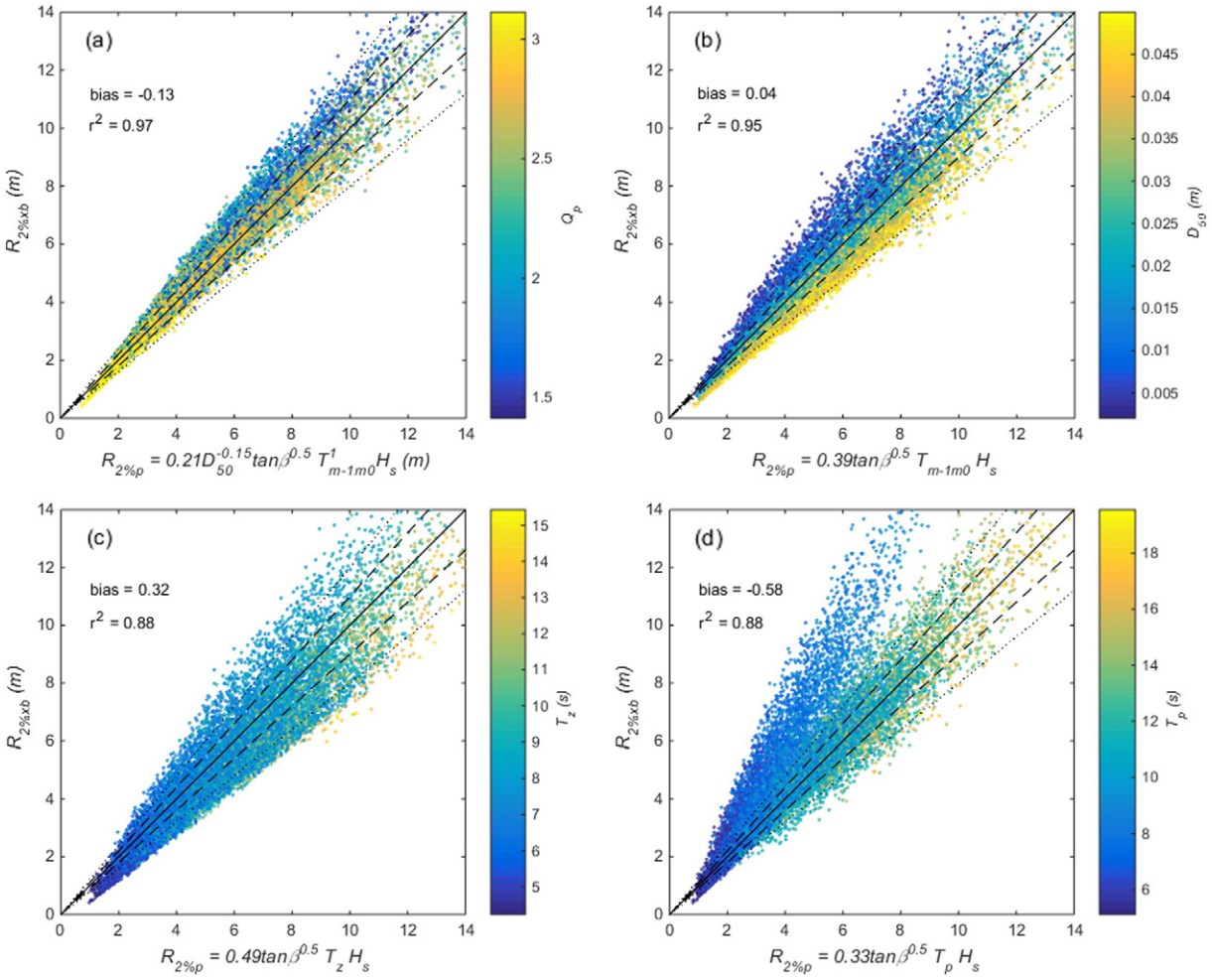

Fig. 13. Runup data ($R_{2\%p}$) obtained with XBeach-G compared with four runup formulae: (a) Eq. (9) (full runup equation); (b) Eq. (10) (runup equation without D_{50}); (c) Eq. (11) (runup equation with T_z instead of $T_{m\text{-}1,0}$, and without D_{50}) and (d) Eq. (12) (runup equation with T_p instead of $T_{m\text{-}1,0}$, and without D_{50}). Black dashed line is the 10% error band while grey dashed line is the 20% error band.

more spread in the data for more energetic conditions. Eq. (12), where C = 0.33, is plotted in Fig. 13d and highlights the main issue of characterising a complex (i.e., bimodal) wave spectrum by the spectral peak period. The modelled runup data appear to fall into 2 clusters, and for neither of these the fit to the whole data set is appropriate. To characterise a bimodal wave spectrum by an appropriate wave period, this parameter must reflect the complete spectrum, were available, and thus involve spectral moments (as in $T_{m-1,0}$ or $T_{m0,1}$).

Eqs. (9)–(12) were applied to the entire runup dataset collected at the four pure gravel beaches (LOB, SLP, CSL, HGI; cf. Fig. 8) and the results are plotted in Fig. 14. Application of the 'full' runup equation (Eq. (9)) to the measured runup dataset (Fig. 14a) shows a good overall fit, characterised by $r^2 = 0.87$ and a bias of 0.35 m. As with Fig. 12, the removal of grain size results in greater spread for lower runup values and over-prediction for more energetic events (Fig. 14b). This trend is made worse by removal of the spectral mean period and use of mean period (Fig. 14c) while use of the peak period results in greater under prediction during low energy conditions (Fig. 14d). The performance of the 'full' runup equation derived from the synthetic data set (Fig. 14a) is not as good as the application of the XBeach-G model (cf. Fig. 9), but is vastly superior to the existing empirical runup equations (cf. Fig. 8).

4. Discussion and conclusions

The development of any empirical equation is strongly dependent on the quality of the data upon which it is based. The field dataset from a range of sites presented here includes information on beach morphology and sedimentology, wave conditions and extreme runup, and all parameters extracted from these measurements are subject to a natural variability, as well as measurement error. Not surprisingly, therefore, considerable scatter remains in the data, even when fitted to the 'best' equation or the XBeach-G model. The largest cause of scatter in the data is considered to be the estimation of the runup elevation from the video data. Apart from pixel resolution and issues with appropriate identification of the leading edge, there is also the assumption that the beach is planar, two-dimensional and stable during the experiment. Additionally, considering the relatively short time series (17 min) and the long wave periods generally encountered under the more energetic wave conditions ($T_p > 10$ s), the 2% runup statistic is often based on only a handful of runup events. Nevertheless, the methodology used is identical to that deployed in the more recent previous runup studies (Aagard and Holm, 1989; Holland and Holman, 1993; Ruessink et al., 1998; Ruggiero et al., 2001; Stockdon et al., 2006).

The reduction in the coefficient of determination (r^2) from fitting the data to the XBeach-G model to fitting the data to the new runup equation (Eq. (9)) is a direct result of the need to express the complex beach profile and incident wave spectrum into simple parameterisations ($\tan\beta$, H_s and T_{m-1m0}). XBeach-G allows the user to define the full inter/sub-tidal profile and the wave spectrum, whereas the empirical runup equation, by design, uses representative slope values and wave parameters that will inherently reduce fit. A validated

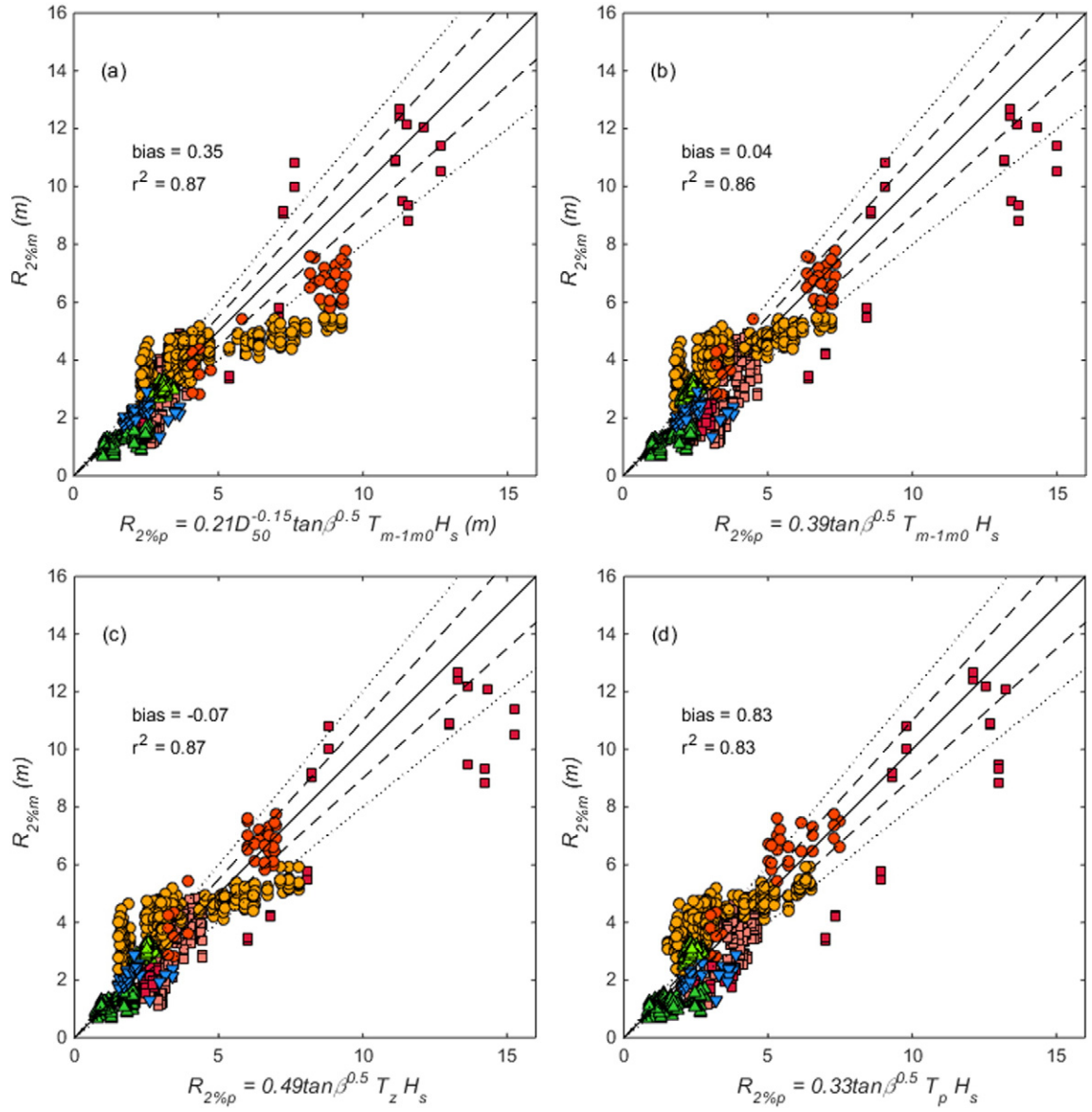

Fig. 14. Comparison of 2% exceedence runup between field measurements at CSL (red squares), LOB (orange circles), SLP (green triangles) and HGI (blue inverted triangles) and (a) Eq. (9) (full runup equation); (b) Eq. (10) (runup equation without D_{50}); (c) Eq. (11) (runup equation with T_z instead of $T_{m\text{-}1,0}$, and without D_{50}) and (d) Eq. (12) (runup equation with T_p instead of $T_{m\text{-}1,0}$, and without D_{50}). Black dashed line is the 10% error band while grey dashed line is the 20% error and. Symbol colours are consistent with Figs. 7, 8 and 9.

numerical model will always outperform an empirical equation; the strength of a runup equation is its convenience.

Application of existing runup formulae to the field data and the synthetic XBeach-G data resulted in a consistent under-prediction of the runup height, especially for the more energetic waves. Of particular note is the under-prediction by the Stockdon, 2006 equation, which is one of the most widely used runup predictors at present, and which under-predicts runup under energetic conditions by over 50%. Underestimation of wave run-up by conventional run-up models (e.g., Stockdon, 2006) has previously also been noted for tsunamis, where similarly to gravel beaches, the surf zone is narrow or non-existent (Baldock et al., 2009). However, Stockdon, 2006 derived their equation using data from sandy beaches with concave beach profile and/or barred surf zones, where wave breaking under energetic wave conditions occurs across an increasingly wide surf zone, limiting wave runup at the beachface. In contrast, the new gravel beach equation is specific to beaches characterised by planar slopes that extend well into the sub-tidal region and which can maintain a reflective morphodynamic condition even under the most energetic conditions. The equations presented in this paper differ from equations based on the wave steepness (e.g., Powell) or Iribarren parameter through the introduction of a dependency on the wave period. While the physical processes related to this dependency are not fully understood, the effect of the introduction of this dependency is greater accuracy in the prediction of wave run-up under energetic conditions. It should be noted that Eqs. (9)–(12) contain a dimensional constant with unit s^{-1}. While these equations fit the range of gravel beach field data and synthetic model data well, the inclusion of a dimensional constant implies that the equations can only be used for conditions similar to those in the field and model data set. Specifically, since the relative wave run-up ($R_{2\%}/H$) scales linearly with the wave period in Eqs. (9)–(12), these empirical equations should not be applicable in the case of Froude-scaled physical model experiments. Further research is recommended to describe the physical processes leading to the dimensionality in the constant, and to use this knowledge to non-dimensionalise future wave run-up equations. As evident in Fig. 1 gravel dominated beaches experience wave breaking at the beachface with no surfzone to dissipate wave energy. This dynamic results in the large runup values we have

measured, especially during storm conditions, supported by the model results. Future work will focus on developing a runup equation that can extend across the entire morphodynamic range, from fully reflective to fully dissipative, possibly involving a wave height-dependent 'effective' beach gradient (Mayer and Kriebel, 1994). The large runups that we have recorded stand alone in the literature for gravel beaches although the relative runup ($R_{2\%}$/H) is not above those measured on steep-sloping structures (~1–3, Van der Meer and Stam, 1992) and on smooth, impermeable beds (~0.5–2.5, Hughes, 2004).

This study has successfully combined the largest dataset of runup on gravel beaches to date with synthetic data generated using the XBeach-G model to produce a new parameterisation for predicting 2% exceedance runup values ($R_{2\%}$). Ten separate field datasets, from six meso-macro tidal field sites in the UK were collected over a 2-year period during energetic conditions (H_s = 1–8 m). Video data were used to characterise runup behaviour and derive runup statistics for a range of beach slopes, grain sizes and wave climates. The results presented show relative runup heights ($R_{2\%}/H_s$) ranging from 0.5 to 1.8, and, in line with previous studies, a good relationship between $R_{2\%}/H_s$ and the Iribarren number. The gravel-specific model XBeach-G was tested against the field data and shown to reproduce the results with a high level of accuracy allowing the original parameter space of the dataset to be expanded with synthetic data runs. Regression analysis of the modelled data helped identify the key parameters, including significant wave height (H_s), spectral mean wave period ($T_{m-1,0}$), beach slope (tanβ) and grain size (D_{50}). The results highlight the importance of beach slope, grain size and the spectral shape which can be lost where peak wave period is used (T_p). For broader application, where spectral wave data is not available, the inclusion of mean wave period provides a suitable replacement particularly at sites where bimodality may be present. A new parameterisation was then developed and tested against both the XBeach-G data and the measured field data showing a vastly improved fit over existing gravel specific runup equations.

Acknowledgments

The authors would like to thank the superb fieldwork staff who were involved with the numerous deployments during storm conditions. Particular thanks go to Mr. Peter Ganderton and Dr. Luis Melo de Almeida for their support and efforts. Thanks are also given to the Engineering and Physical Science Research Council (EPSRC) through which this study was funded (EP/H040056/1) in partnership with The Channel Coastal Observatory, The Environment Agency and HR Wallingford. This project was also supported and benefited from a separate EPSRC project; Adaptation and Resilience of the UK Energy System to Climate Change (ARCoES; EP/1035390/1). We also thank our reviewers who provided constructive and helpful input into the final manuscript.

Appendix A. Runup equations used in this study

Source	Equation	Variables	
Stockdon et al. (2006)	$R_{2\%} = 1.1(0.35tan\beta(H_0/\lambda_0)^{1/2} + \frac{[H_0/\lambda_0(0.563tan\beta^2+0.004)]^{1/2}}{2})$	λ_0 = deep water wave length of the peak period wave	Eq. (A1)
Van der Meer and Janssen (1994)	$R_{2\%} = H_s$ 1.6 $\gamma_h\gamma_f\gamma_\beta\xi_{eq}$ $\xi_{op} = tan\beta/\sqrt{2\pi H_s/(gT_p^2)}$	γb = reduction factor (rf) for a berm γh = rf for a shallow foreshore γf = rf for slope roughness $\gamma\beta$ = rf for oblique wave attack ξ_{eq} = equivalent breaker parameter for a slope with a berm $\xi_{eq} = \gamma b\ \xi_{op}$	Eq. (A2) Eq. (A3)
Polidoro et al. (2013)	$R_{2\%} = 1.04\ H_{m0}(\frac{T_{m-1,0}}{T_{m0,2}})^{0.5}\xi_{m-1,0}{}^{0.5}\ (Exp(-Q_P))^{0.5} + (0.095H_{m0}{}^{0.5}L_{m-1,0}{}^{0.5})$	Q_P = peakedness parameter (Goda, 1976)	Eq. (A4)
Powell (1990)	$H_c = H_s[2.86-62.69\ (\frac{H_s}{L_0}) + 443.29\ (\frac{H_s}{L_0})^2]$ $R_{2\%} = H_c(-\frac{.\ln 0.02}{4.2})^{0.455}$	H_c = crest position (runup position) L_0 = mean deep water wave length	Eq. (A5)

References

Aagard, T., Holm, J., 1989. Digitization of wave runup using video records. J. Coast. Res. 5, 547–551.
Aminti, P., Cipriani, L.E., Pranzini, E., 2003. Back to the beach: converting seawalls into gravel beaches. In: Goudas, C., Katsiaris, G., May, V., Karambas, T. (Eds.), Soft Shore Protection. Vol. 7 of Coastal Systems and Continental Margins. Springer, Netherlands, pp. 261–274.
Austin, M.J., Buscombe, D., 2008. Morphological change and sediment dynamics of the beach step on a macrotidal gravel beach. Mar. Geol. 249 (3-4), 167–183.
Baldock, T.E., Cox, D., Maddux, T., Killian, J., Fayler, L., 2009. Kinematics of breaking tsunami wavefronts: a data set from large scale laboratory experiments. Coast. Eng. 56 (5–6), 506–516.
Austin, M.J., Masselink, G., 2006. Observations of morphological change sediment transport on a steep gravel beach. Mar. Geol. 229, 59–77.
Austin, M.J., Masselink, G., McCall, R.T., Poate, T.G., 2013. Groundwater dynamics in coastal gravel barriers backed by freshwater lagoons and the potential for saline intrusion: two cases from the UK. J. Mar. Syst. 123–124 (0), 19–32.
Battjes, J.A., 1974. Surf Similarity, 14th International Conference of Coastal Engineerings. ASCE, pp. 466–480.
Battjes, J.A., 1971. Run-up distributions of waves breaking on slopes. Journal of the waterways, harbors and coastal engineering division 97 (1), 91–114.
Bradbury, A.P., Mason, T.E., Poate, T., 2007. Implications of the spectral shape of wave conditions for engineering design and coastal hazard assessment - evidence from the English Channel. Presented at the 10th International Workshop on Wave Hindcasting and Forecasting, 11–16 Nov. 2007, Oahu, Hawaii.
Goda, Y., 1976. On wave groups. Proceedings, Behaviour of Offshore Structures Conference, Trondheim. vol. 1, pp. 115–128.
Guza, R.T., Inman, D.L., 1975. Edge waves and beach cusps. J. Geophys. Res. 80 (21), 2997–3012.
Guza, R.T., Thornton, E.B., 1982. Swash oscillations on a natural beach. J. Geophys. Res. 87 (C1), 483–491.
Hazen, A., 1892. Some physical properties of sands and gravels, with special reference to their use in filtration. Pub. Doc. 34, Massachusetts State Board of Health. 24th Annual Report. Publication No. 34, pp. 539–556.
Heijne, I., West, G., 1991. Chesil sea defence scheme. Paper 2: design of interceptor drain. Proc. Inst. Civ. Eng. 90, 799–817.
Holland, K.T., Holman, R.A., 1993. The statistical distribution of swash maxima on natural beaches. J. Geophys. Res. 98, 10271–10278.
Holland, K.T., Raubenheimer, B., Guza, R.T., Holman, R.A., 1995. Runup kinematics on a natural beach. Journal of Geophysical Research: Oceans 100 (C3), 4985–4993.
Holland, K.T., Holman, R.A., Lippmann, T.C., Stanley, J., Plant, N., 1997. Practical use of video imagery in nearshore oceanographic field studies. Oceanic Engineering, IEEE Journal of 22 (1), 81–92.
Holman, R.A., Guza, R.T., 1984. Measuring run-up on a natural beach. Coast. Eng. 8 (2), 129–140.
Holman, R.A., Sallenger Jr., A.H., 1985. Setup and swash on a natural beach. J. Geophys. Res. 90 (C1), 945–953.
Holman, R.A., 1986. Extreme value statistics for wave run-up on a natural beach. Coast. Eng. 9 (6), 527–544.
Nielsen, P., Hanslow, D.J., 1991. Wave runup distributions on natural beaches. J. Coast. Res. 7 (4), 1139–1152.

Hughes, M.G., Cowell, P.J., 1987. Adjustment of reflective beaches to waves. J. Coast. Res. 3 (2), 153–167.
Hughes, S.A., 2004. Estimation of wave run-up on smooth, impermeable slopes using the wave momentum flux parameter. Coast. Eng. 51 (11–12), 1085–1104 (December 2004, ISSN 0378-3839).
Ivamy, M.C., Kench, P.S., 2006. Hydrodynamics and morphological adjustment of a mixed sand and gravel beach, Torere, Bay of Plenty, New Zealand. Mar. Geol. 228, 137–152.
Jennings, R., Shulmeister, J., 2002. A field based classification scheme for gravel beaches. Mar. Geol. 186 (3–4), 211–228.
Johnson, C.N., 1987. Rubble beaches versus rubble revetments. Proceedings ASCE Conference on Coastal Sediments 1987. American Society of Civil Engineers, Reston, Virginia, USA, pp. 1216–1231.
Masselink, G., McCall, R.T., Poate, T., Van Geer, P., 2014. Modelling storm response on gravel beaches using XBeach-G. Proceedings of the ICE - Maritime Engineering. vol. 167 (4), pp. 173–191.
Masselink, G., Scott, T., Poate, T., Russell, P., Davidson, M., Conley, D., 2015. The extreme 2013/14 winter storms: Hydrodynamic forcing and coastal response along the southwest coast of England. Earth Surf. Processes Landforms http://dx.doi.org/10.1002/esp.3836.
Matias, A., Williams, J.J., Masselink, G., Ferreira, Ó., 2012. Overwash threshold for gravel barriers. Coast. Eng. 63 (0), 48–61.
Mayer, R.H., Kriebel, D.L., 1994. Wave runup on composite-slope and concave beaches. Proceedings of the 24th Coastal Engineering Conference, ASCE, pp. 2325–2339.
McCall, R.T., Masselink, G., Poate, T., Roelvink, J.A., Almeida, L.P., Davidson, M., Russell, P.E., 2014. Modelling storm hydrodynamics on gravel beaches with XBeach-G. Coast. Eng. 91, 231–250.
McCall, R.T., Masselink, G., Poate, T.G., Roelvink, J.A., Almeida, L.P., 2015a. Modelling the morphodynamics of gravel beaches during storms with XBeach-G. Coast. Eng. 103, 52–66.
McCall, R., Masselink, G., Poate, T., Roelvink, J., 2015b. Modelling gravel barrier resilience during storms with XBeach-G: the role of infiltration. In: Wang, P., Rosati, J.D., Cheng, J. (Eds.), Proceedings of Coastal Sediments Conference. World Scientific, San Diego, USA.
Orford, J.D., Carter, R.W.G., 1982. Crestal overtop and washover sedimentation on a fringing sandy gravel barrier coast, Carnsore Point, SE Ireland. J. Sediment. Petrol. 52, 265–278.
Orford, J.D., Carter, R.W.G., Forbes, D.L., 1991. Gravel barrier migration and sea level rise; some observations from Story Head, Nova Scotia, Canada. J. Coast. Res. 7, 477–488.
Orford, J.D., Jennings, S.C., Pethick, J., 2003. In: Davis, R.A. (Ed.), Extreme storm effect on gravel-dominated barriers. Coastal sediments '03. Proceedings of the International Conference on Coastal Sediments, p. 2003.
Ruggiero, P., Komar, P.D., McDouglas, W.G., Marra, J.J., 2001. Wave runup, extreme water levels and erosion of properties backing beaches. J. Coast. Res. 17 (2), 407–419.
Poate, T.G., Masselink, G., Davisdon, M., McCall, R., Russell, P., Turner, I., 2013. High frequency in-situ field measurements of morphological response on a fine gravel beach during energetic wave conditions. Mar. Geol. 342, 1–13. http://dx.doi.org/10.1016/j.margo.2013.05.009.
Polidoro, A., Dornbusch, U., Pullen, T., 2013. Improved maximum run-up formula for mixed beaches based on field data. ICE Coasts, Marine Structures and Breakwaters Conference, Edinburgh, pp. 389–398.
Powell, K.A., 1990. Predicting Short Term Profile Response for Shingle Beaches. Hydraulics Research Limited, Wallingford, Oxfordshire. Report SR2 19.
Roelvink, D., Reniers, A., van Dongeren, A., van Thiel de Vries, J., McCall, R., Lescinski, J., 2009. Modelling storm impacts on beaches, dunes and barrier islands. Coast. Eng. 56 (11-12), 1133–1152.
Ruessink, B.G., Kleinhaus, M.G., van den Beukel, P.G.L., 1998. Observations of swash under highly dissipative conditions. J. Geophys. Res. 103 (C2), 3111–3118.
Roos, A., Battjes, J.A., 1976. Characteristics of Flow in Run-Up of Periodic Waves. Coastal Engineering. 1, pp. 781–795.
Ruiz de Alegria-Arzaburu, A., Masselink, G., 2010. Storm response and beach rotation on a gravel beach, Slapton Sands, U.K. Mar. Geol. 278 (1–4), 77–99.
Senechal, N., Coco, G., Bryan, K.R., Holman, R.A., 2011. Wave runup during extreme storm conditions. J. Geophys. Res. 116, C07032. http://dx.doi.org/10.1029/2010JC006819.
Stockdon, H.F., Sallenger, J.A.H., Holman, R.A., Howd, P.A., 2007. A simple model for the spatially-variable coastal response to hurricanes. Mar. Geol. 238 (1–4), 1–20. http://dx.doi.org/10.1016/j.margeo.2006.11.004 (ISSN 0025-3227).
Stripling, A., Bradbury, A.P., Brampton, A.H., Cope, S.N., 2008. Understanding Barrier Beaches Joint DEFRA/EA Flood and Coastal Erosion Risk Management R&D Programme. Technical Report FD1924/TR.
Van der Meer, J.W., Stam, C.J.M., 1992. Wave runup on smooth and rocky slopes of coastal structures. J. Waterw. Port Coast. Ocean Eng. 534–550 http://dx.doi.org/10.1061/(ASCE)0733-950X(1992)118:5(534).
Van der Meer, J.W., Janssen, J.P.F.M., 1994. Wave Run-up and Wave Overtopping at Dikes and Revetments. Delft Hydraulics Publication No. 485.